

# Synthesis and Visualization of a Core Cross-Linked Star Polymer Carrying Optically Active Rigid-Rod Helical Polyisocyanide Arms and Its Chiral Recognition Ability

Toshitaka Miyabe, Hiroki Iida, Motonori Banno, Tomoko Yamaguchi, and Eiji Yashima\*

Department of Molecular Design and Engineering, Graduate School of Engineering, Nagoya University, Chikusa-ku, Nagoya 464-8603, Japan

 Supporting Information

## INTRODUCTION

Star polymers, a class of branched polymers, have attracted great attention over the past few decades because of their greater accessibility by well-established living polymerization techniques, structural diversity in three-dimensional (3D) core-shell architectures, and unique properties and functions being different from those of the corresponding linear counterparts.<sup>1</sup> Living ionic and radical polymerizations of monomers followed by cross-linking with a difunctional comonomer (“arm-first” approach)<sup>2</sup> have frequently been employed for the design and synthesis of star polymers consisting of a densely cross-linked core and linear radiating multiple arms, which enables us to produce star polymers bearing specific functions,<sup>1b</sup> such as a catalytic activity<sup>3</sup> and molecular recognition ability,<sup>4</sup> by introducing the desired functional groups at the core or the arm segments. Although a variety of star polymers with a varying number of arms, chemical compositions, and functional groups have been prepared, most of the star polymers prepared to date are optically inactive.<sup>1</sup> Optically active star polymers, in particular those carrying rodlike one-handed helical arms,<sup>4b,5</sup> are quite rare in spite of their potential in practical applications as novel chiral materials for enantioselective catalysis and adsorbents<sup>6</sup> because of their unique helix-bundle structures generated by self-assembled helical arms, which may provide confined chiral environments for the efficient chiral recognition of enantiomers and chiral polymers.

To this end, we have synthesized a novel optically active star polymer (*M*-poly-*L*-1(–)-*b*-3) bearing rodlike helical polyisocyanide arms based on the “arm-first” approach (Figure 1). Our design approach builds upon our previous findings that both right (*P*)- and left (*M*)-handed helical polyisocyanides with a different molecular weight (MW) and a narrow molecular weight distribution (MWD) (*P*- and *M*-poly-*L*-1s, respectively) can be obtained by the living polymerization of an enantiomerically pure phenyl isocyanide bearing an *L*-alanine pendant with a long *n*-decyl chain (*L*-1) using the  $\mu$ -ethynediyl Pt–Pd catalyst (**2**),<sup>7</sup> followed by the facile fractionation with acetone (Figure 1).<sup>8,9</sup> The fractionated single-handed helical polyisocyanides (*P*- and *M*-poly-*L*-1s)<sup>10</sup> as revealed by high-resolution atomic force microscopy (AFM)<sup>8</sup> maintained their living feature and can be used as an initiator (macroinitiator) for the further block copolymerizations of isocyanides.<sup>11</sup> The polyisocyanides possess an unprecedented long persistence length of 220 nm stabilized by intramolecular hydrogen-bonding networks through

the neighboring amide N–H groups.<sup>12</sup> Because of the anomalous stiff backbones of the helical polyisocyanides, we anticipated that the resulting star polymer would form a unique star-shaped “spiny” architecture and their topologically interesting individual molecular structures including the shape, the molecular lengths and numbers of arms, and the helical structures of the arms (helical pitch, helical sense (*P* or *M*), and helical sense excess as well) might be directly visualized by AFM. Although AFM has become a powerful tool to study a variety of polymer materials, such as star and branched polymers,<sup>13</sup> the visualization of the branching topology of star polymers is still challenging and their real images of topological structures remain difficult to observe,<sup>14</sup> except for star polymers carrying three or four polymer brushes as the arms or those prepared by uniform-arm macroinitiators<sup>14b,15</sup> mainly because many flexible arms attached to a central core fold into condensed random coils in an overlapping interdigitated manner, leading to complicated images.

## RESULTS AND DISCUSSION

The optically active star polymer (*M*-poly-*L*-1(–)-*b*-3) was prepared by cross-linking of the living left-handed helical *M*-poly-*L*-1(–) (the number-average molecular weight ( $M_n$ ) and its distribution were  $M_n = 6.00 \times 10^4$  and  $M_w/M_n = 1.06$ , respectively)<sup>8,11</sup> with a cross-linker **3** (0.1 equiv based on the monomer units of *M*-poly-*L*-1(–)) in tetrahydrofuran (THF) at 55 °C. The cross-linking reaction, the progress of which was monitored by IR, was terminated after **3** had been completely consumed. Because the obtained core cross-linked star polymer carrying the rigid-rod helical arms contained a small amount of the unreacted macroinitiator (*M*-poly-*L*-1(–), ca. 11%), the polymer was purified by the recycling preparative size exclusion chromatography (SEC), yielding the higher MW star polymer (*M*-poly-*L*-1(–)-*b*-3); the composition (*m* and *n* in Figure 1) was calculated to be *m*:*n* = 1:9 based on the conversion of **3** and *M*-poly-*L*-1(–), since the NMR of the star polymer was too broad to determine the composition. The  $M_n$  and the absolute weight-average molecular weight ( $M_w$ ) of the star polymer were determined to be  $5.79 \times 10^5$  and  $1.11 \times 10^6$ , respectively, by multiangle light scattering (MALS) coupled

Received: September 2, 2011

Revised: September 27, 2011

Published: October 07, 2011

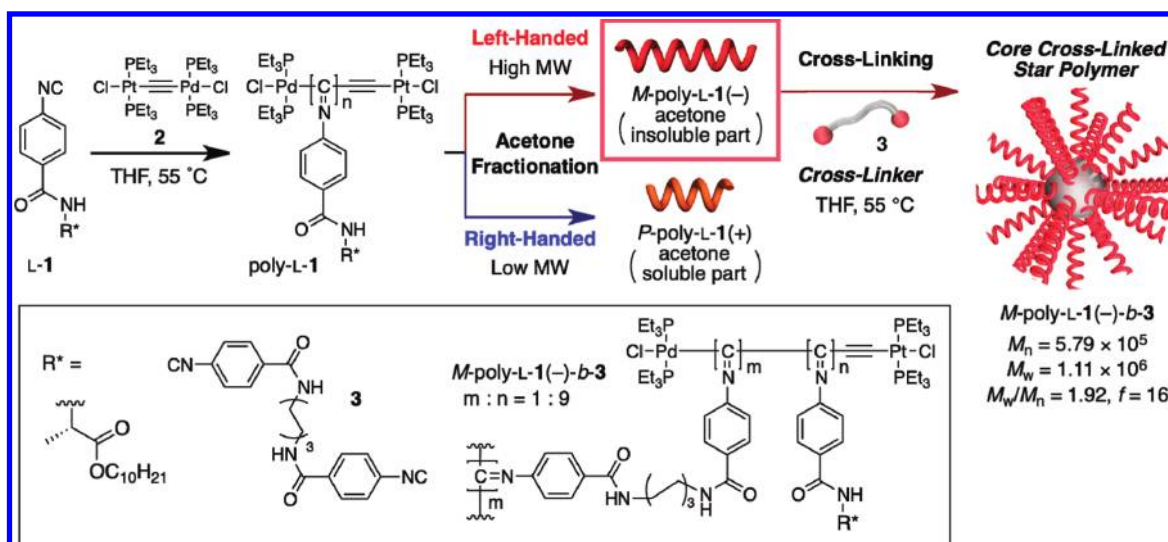


**Figure 1.** Schematic illustration of the synthesis of a star polymer  $M$ -poly- $L$ -1(-)- $b$ -3. The helix-sense-selective living polymerization of  $L$ -1 with the  $\mu$ -ethynediyl Pt–Pd catalyst (2) gives a mixture of diastereomeric, right-handed, and left-handed helical poly- $L$ -1s with different MWs and a narrow MWD, which can be further separated into the right- and left-handed helical poly- $L$ -1s by fractionation with acetone. Left-handed helical  $M$ -poly- $L$ -1(-) was used as the macroinitiator for further cross-linking reaction with the cross-linker 3, yielding a star polymer  $M$ -poly- $L$ -1(-)- $b$ -3.

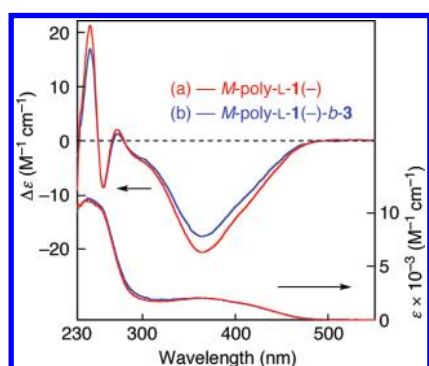


**Figure 2.** CD and absorption spectra of  $M$ -poly- $L$ -1(-) (a) and  $M$ -poly- $L$ -1(-)- $b$ -3 (b) in chloroform (0.2 mg/mL) at 25 °C.

with SEC, and thus the number of arms ( $f$ ) was calculated to be 16.<sup>16</sup>

Figure 2 shows the CD and absorption spectra of the macroinitiator ( $M$ -poly- $L$ -1(-)) and star polymer ( $M$ -poly- $L$ -1(-)- $b$ -3) in chloroform at 25 °C. The first Cotton effect intensity of  $M$ -poly- $L$ -1(-)- $b$ -3 ( $\Delta\epsilon_{364} = -17.7$ ) at 364 nm, which reflects a helical sense excess of the polymer backbone,<sup>8,11</sup> slightly decreased (ca. 14%) after the cross-linking reaction of  $M$ -poly- $L$ -1(-) ( $\Delta\epsilon_{364} = -20.6$ ) with achiral 3, suggesting that the core units derived from 3 may not have a preferred-handed helical conformation, but the left-handed helical conformation of  $M$ -poly- $L$ -1(-) was almost completely retained after the block copolymerization.

Figure 3 shows the AFM images of the isolated  $M$ -poly- $L$ -1(-) and  $M$ -poly- $L$ -1(-)- $b$ -3 molecules prepared by casting a dilute chloroform solution on mica. Individual rodlike linear macroinitiator chains with a number-average height ( $H_n$ ) of ca. 1.2 nm were clearly observed (Figure 3A), while the star polymers showed a unique “spiny”-shape topology with varying rodlike arms attached to a cross-linked central core and the rodlike arms of the number-average molecular length of ca. 14 nm tend to

assemble to form a helix-bundle structure on a hydrophilic mica substrate (Figure 3B,C); thereby the number of arms may be underestimated (Figure 3C).

Based on an evaluation of more than 100 star polymers including Figure 3B,C, the number-average diameter ( $D_n$ ), the weight-average diameter ( $D_w$ ), and its distribution ( $D_w/D_n$ ) were estimated to be  $39 \pm 10$  nm,  $42 \pm 10$  nm, and 1.07, respectively (Figure S4A). These values were measured without compensation for the tip radius of curvature (ca. 10 nm), and the measured values might be overestimated by around 10 nm because of the broadening effect of the tip. The number-average molecular height ( $H_n = 2.5$  nm), the weight-average molecular height ( $H_w = 3.0$  nm), and the height distribution ( $H_w/H_n = 1.17$ ) of the star polymers were also estimated (Figure S4B).

Previously, we found that rigid-rod helical polyisocyanides<sup>8,11</sup> including  $P$ - and  $M$ -poly- $L$ -1s self-assembled to form regular two-dimensional (2D) helix bundles on a highly oriented pyrolytic graphite (HOPG) substrate after organic solvent vapor exposures, which allows the visualization of the helical structures. We then applied this procedure to the star polymer consisting of the identical  $M$ -poly- $L$ -1(-) as the arms.<sup>17</sup>

Figure 4A shows the typical AFM images of the star polymer,  $M$ -poly- $L$ -1(-)- $b$ -3, deposited on HOPG from a dilute chloroform solution followed by chloroform vapor exposure at ambient temperature for 12 h. Interestingly, the star polymer also self-assembled to form regular 2D monolayers in a hexagonal-like arrangement reflecting the crystallographic structure of the HOPG substrate, in which individual molecules are clearly resolved as densely packed stars. Since the rodlike arms with a constant length form regular helix-bundle structures within a star and between the stars as seen in Figure 4B, the high-resolution AFM measurements allowed the number of arms in the individual star polymers ( $f = 8.9 \pm 3.3$ ) (Figure 4C) and its distribution (Figure 4F) to be obtained. In addition, the left-handed helical structure of the arms with a helical pitch of  $1.33 \pm 0.10$  nm (Figure 4D,E) was clearly observed. The observed helical sense and helical pitch of the arms fairly agreed with those previously

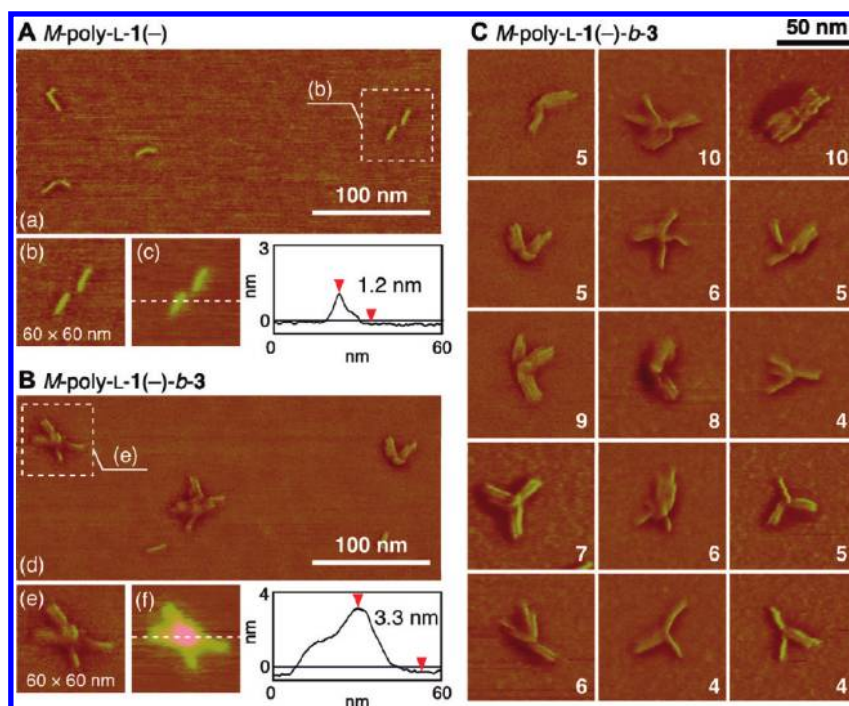
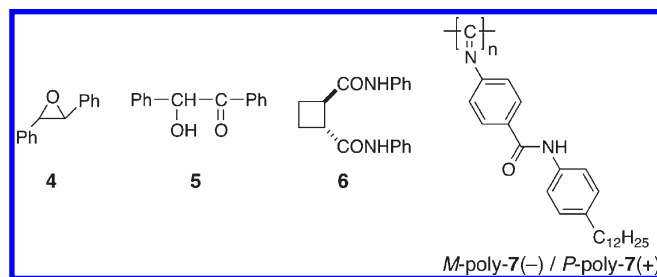


**Figure 3.** AFM phase (a, b, d, e) and height (c, f) images of *M*-poly-*L*-1(-) (A) and *M*-poly-*L*-1(-)-*b*-3 (B) prepared by casting a dilute solution in chloroform (0.001 mg/mL) on mica. The cross-sectional profile denoted by a white dashed line is also shown in (c, f). (C) AFM phase images (scale 80 nm × 80 nm) of *M*-poly-*L*-1(-)-*b*-3 carrying various arms on mica. The number of arms is indicated in each image.

determined for its homopolymer (*M*-poly-*L*-1(-)),<sup>8</sup> whereas the average number of arms of the star polymers estimated by AFM on HOPG was lower than that obtained by the SEC-MALS measurement results ( $f = 16$ ). This disagreement may be ascribed to overlapping of the arms on the HOPG, in particular, for star polymers carrying a higher number of arms. Nevertheless, these AFM results emphasize a novel core cross-linked star polymer bearing stiff helical arms with a controlled helical sense and a constant length that provides almost the entire structural and topological information on the star polymers that involves the molecular shape and branching arm topology of individual star polymers, such as the number and length of the arms and its handedness (helicity) by high-resolution AFM. Such a molecular level visualization except for the helicity is possible only for densely grafted brushlike star polymers prepared by uniform-arm macroinitiators.<sup>14b,15</sup>

The chiral recognition ability of the star polymer, *M*-poly-*L*-1(-)-*b*-3, was then investigated for the racemates (4–6) and a racemic helical polyisocyanide bearing no chiral pendants using the enantioselective adsorption technique (Table 1 and Supporting Information).<sup>18</sup> The star polymer preferentially adsorbed one of the enantiomers of 4–6, furnishing 23, 6.1, and 11% enantiomeric excess (ee), respectively. Based on the amounts and ee values of the analytes remaining in the supernatants during the enantioselective adsorption with the star polymer, the separation factor ( $\alpha$ ), which is a useful measure to evaluate the chiral recognition ability of chiral hosts toward racemic analytes in chiral HPLC, was calculated to be 1.81, 1.20, and 1.45 for 4, 5, and 6, respectively (Table 1). These values are high enough for the almost complete separation of enantiomers when used as a CSP for HPLC, indicating that the star polymer possesses a chiral recognition ability for small racemic molecules. It should be noted that the compounds 4 and 5 were enantioselectively adsorbed better on the star polymer than on the macroinitiator

(*M*-poly-*L*-1(-)), although the compound 6 was resolved slightly better on *M*-poly-*L*-1(-) (Table 1).<sup>10</sup>



Racemic helical polyisocyanides (*M*-poly-7(-) and *P*-poly-7(+)), which had been prepared by a previously reported method based on the “*helicity induction and memory strategy*”<sup>19</sup> followed by modification of the side groups (Supporting Information),<sup>19c,e,f</sup> was then employed as an analyte. Interestingly, *P*-poly-7(+) was helix-sense selectively adsorbed on the star polymer carrying the opposite left-handed helical arms with a moderate enantioselectivity ( $\alpha = 1.14$ ), whereas the corresponding macroinitiator showed a poor chiral recognition ( $\alpha = 1.03$ ) (Table 1, entry 4, and Supporting Information). This helix-sense selective adsorption of racemic helices may have taken place as a result of a confined chiral space created by the intermolecularly self-assembled bundled helical arms of the star polymers, within which a large macromolecule with a preferred-handed helicity could be selectively encapsulated.

## CONCLUSIONS

In conclusion, we have prepared a novel optically active star polymer bearing rigid-rod one-handed helical polyisocyanide

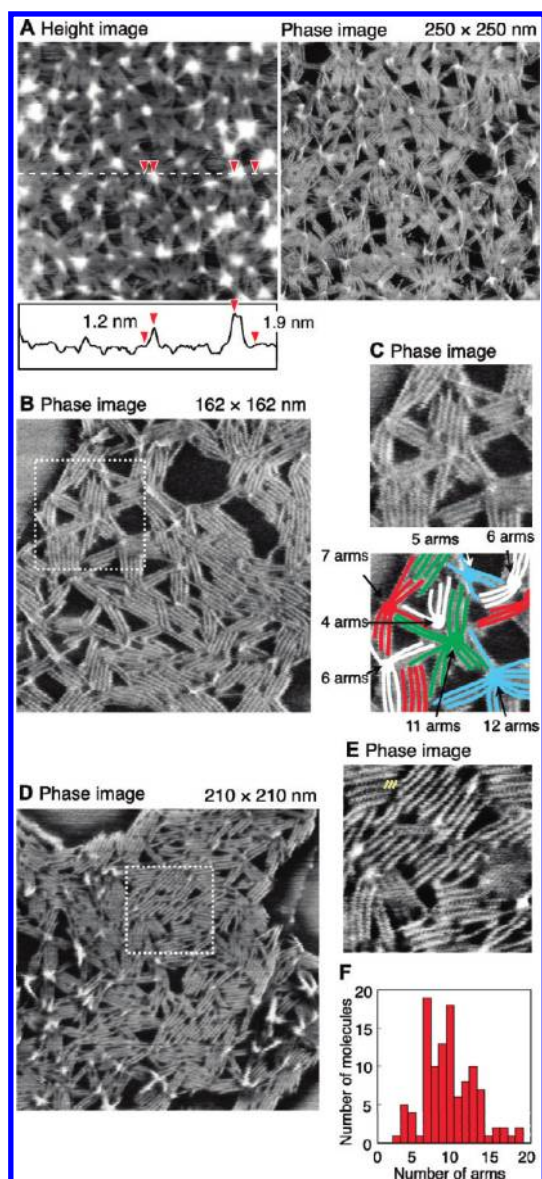


**Figure 4.** (A) AFM height (left) and phase (right) images (scale 250 nm  $\times$  250 nm) of 2D self-assembled *M*-poly-L-1(-)-*b*-3 on HOPG. The samples were prepared by depositing a dilute chloroform solution (0.02 mg/mL), followed by exposure to chloroform vapor for 12 h at ambient temperature (ca. 25 °C). The cross-sectional profile denoted by a white dashed line is also shown. (B) AFM phase image (scale 162 nm  $\times$  162 nm) of 2D self-assembled *M*-poly-L-1(-)-*b*-3 on HOPG. Zoomed AFM image corresponding to the area indicated by a white square is shown in (C). Schematic representations of possible helix-bundle arrangements are also shown (bottom). Each molecule is indicated by different colors. (D) AFM phase image (scale 210 nm  $\times$  210 nm) of 2D self-assembled *M*-poly-L-1(-)-*b*-3 on HOPG. Zoomed AFM image corresponding to the area indicated by a white square is shown in (E). The yellow oblique lines indicate the left-handed helical array of the pendants. (F) Histogram of distribution of the number of arms of *M*-poly-L-1(-)-*b*-3 obtained from AFM images taken from more than 100 molecules.

arms by the copolymerization of the rodlike polyisocyanide macroinitiator with a bifunctional cross-linking agent. The star-shaped “spiny” structure with individual helical arms including the number and length of the arms and its handedness has been

directly visualized by high-resolution AFM. The chiral adsorption experiments revealed the potential of this topologically unique star polymer for separating not only small molecules with a point chirality but also large molecules with a macromolecular helicity. These findings will be useful for developing further topologically unique optical active star polymers with specific functions as chiral materials.

## MATERIALS AND METHODS

**Materials.** 4-Isocyanobenzoyl-L-alanine decyl ester (*L*-1),<sup>8,12,17b</sup> the  $\mu$ -ethynediyl Pt–Pd complex (**2**),<sup>7</sup> and optically active right- and left-handed helical poly(phenyl isocyanide)s with macromolecular helicity memory (*P*-poly-7(+) and *M*-poly-7(-), respectively)<sup>19</sup> were prepared according to the reported methods. The solvents used in the chromatographic experiments were of HPLC grade. The racemates were commercially available or were prepared by the usual methods.<sup>20</sup>

**Synthesis of Star Polymers.** The right- and left-handed helical poly(phenyl isocyanide)s (*P*-poly-L-1(+) and *M*-poly-L-1(-)) were prepared in a similar way to that previously reported (Figure 1).<sup>8</sup> The polymerization of *L*-1 (2.00 g, 5.60 mmol) was carried out in a dry glass ampule under a dry nitrogen atmosphere in THF using **2** ( $[1]/[2] = 100$ ) as the catalyst at 55 °C for 20 h. The obtained poly-L-1 (1.86 g, 93% yield) was then fractionated with acetone into high-MW left-handed helical *M*-poly-L-1(-) and low-MW right-handed helical *P*-poly-L-1(+) in 62 and 13% yield, respectively (Figure 1). The  $M_n$  and  $M_w/M_n$  were  $1.18 \times 10^5$  and 1.09 (*M*-poly-L-1(-)) and  $6.74 \times 10^4$  and 1.08 (*P*-poly-L-1(+)), respectively, determined by SEC with polystyrene standards and THF containing 0.1 wt % tetra-*n*-butylammonium bromide (TBAB) was used as the eluent at the flow rate of 1.0 mL/min. The resulting *M*-poly-L-1(-) was further used as the macroinitiator. The  $M_n$  and  $M_w$  of *M*-poly-L-1(-) as determined by SEC-MALS measurements were  $6.00 \times 10^4$  and  $6.38 \times 10^4$ , respectively.

A solution of the cross-linking monomer **3** (12.6 mg, 0.0336 mmol) in dimethylformamide (DMF) (0.8 mL) was added to a solution of *M*-poly-L-1(-) (120 mg, 0.335 mmol) in THF (2.6 mL), and the mixture was then stirred under a dry nitrogen atmosphere and heated to 55 °C. After 20 h, the resulting star polymer (*M*-poly-L-1(-)-*b*-3) was precipitated into a large amount of methanol (50 mL), collected by centrifugation, and dried in vacuo at room temperature overnight. The star polymer was further fractionated by the recycling preparative SEC to remove the unreacted macroinitiator, yielding the higher MW star polymer (23.8 mg, 18% yield) (Figure 1). The SEC measurement revealed that the purified star polymer contained the macroinitiator of less than 1 mol % after the recycling preparative SEC. The  $M_n$  and  $M_w/M_n$  of the fractionated star polymer were  $9.40 \times 10^5$  and 1.10, respectively, as determined by SEC with polystyrene standards and THF containing 0.1 wt % TBAB was used as the eluent at the flow rate of 1.0 mL/min. The  $M_n$  and  $M_w$  of the star polymer were also measured by SEC-MALS and were  $5.79 \times 10^5$  and  $1.11 \times 10^6$ , respectively. The number of arms per molecule ( $f$ ) was then calculated to be 16 according to the equation  $f = (\text{weight fraction of arm}) \times M_w(\text{star})/M_w(\text{arm})$ .<sup>16</sup>

Spectroscopic data of *M*-poly-L-1(-)-*b*-3: IR (film,  $\text{cm}^{-1}$ ): 3278 ( $\nu_{\text{N-H}}$ ), 1747 ( $\nu_{\text{C=O}}$  ester), 1633 (amide I), 1536 (amide II). <sup>1</sup>H NMR ( $\text{CDCl}_3$ , 55 °C, 500 MHz):  $\delta$  0.87 (broad,  $\text{CH}_3$ , 3H), 1.25 (broad,  $\text{CH}_2$ , 14.4H), 1.53 (broad,  $\text{CH}_3$  and  $\text{CH}_2$ , 5.4H), 3.30–4.30 (broad,  $\text{CH}_2$ , 2.4H), 4.30–4.80 (broad, CH, 1H), 4.80–7.80 (broad, aromatic, 4.9H), 8.00–9.00 (broad, NH, 1.2H).  $[\alpha]_{\text{D}}^{20} -1553$  ( $c$  0.1, chloroform). Anal. Calcd (%) for  $(\text{C}_{21}\text{H}_{30}\text{N}_2\text{O}_3)_9(\text{C}_{22}\text{H}_{22}\text{N}_4\text{O}_2)_1(\text{H}_2\text{O})_{3.2}$ : C, 69.27; H, 8.22; N, 8.42. Found: C, 69.22; H, 8.10; N, 8.42.

**Typical Procedure for Enantioselective Adsorption of Small Chiral Compounds.** A typical experimental procedure is described below. The star polymer, *M*-poly-L-1(-)-*b*-3 (16.0 mg), was thoroughly washed with a hexane–2-propanol mixture (90:10, v/v)

**Table 1. Enantioselective Adsorption of Racemic Compounds (4–6) and Helical Polymer (Poly-7) on *M*-Poly-L-1(–)-b-3<sup>a</sup>**

entry	analyte	yield ( <i>ee</i> ) of adsorbed analyte <sup>b</sup> (%)	<i>ee</i> of free analyte in solution <sup>b</sup> (%)	separation factor <sup>c</sup> ( $\alpha$ )	separation factor ( $\alpha$ ) of <i>M</i> -poly-L-1(–) <sup>d</sup>
1 <sup>e</sup>	4	22.0 ± 0.4 (23 ± 1 (–))	6.5 ± 0.3 (+)	1.81 ± 0.05 (+)	1.70 (+)
2 <sup>e,f</sup>	5	34.6 ± 1.9 (6.1 ± 0.7(+))	3.2 ± 0.3 (–)	1.20 ± 0.02 (–)	1.10 (–)
3 <sup>e,g</sup>	6	42.4 ± 2.2 (11 ± 1 (–))	7.9 ± 0.5 (+)	1.45 ± 0.02 (+)	1.53 (+)
4 <sup>h</sup>	<i>M</i> -poly-7(–)/ <i>P</i> -poly-7(+)	6.91 <sup>i</sup> (6.0 (+)) <sup>ij</sup>	0.45 (–) <sup>j</sup>	1.14 (–)	1.03 (–) <sup>k</sup>

<sup>a</sup> Experimental conditions: *M*-poly-L-1(–)-b-3 16.0 mg; analyte 0.005 mg (200  $\mu$ L portion from a 0.025 mg/mL solution in hexane–2-propanol (98:2, v/v)). <sup>b</sup> Determined by HPLC analysis of the supernatant solution using a Chiralcel OD-H column; eluent, hexane–2-propanol (90:10, v/v); flow-rate, 0.5 mL/min. <sup>c</sup> Calculated according to the equation  $\alpha = (F_{\text{major}}(\%)/F_{\text{minor}}(\%))/(A_{\text{major}}(\%)/A_{\text{minor}}(\%))$ , where  $F_{\text{major}}$  and  $F_{\text{minor}}$  are the percentages of major and minor enantiomers of free analyte in the supernatant solutions, respectively, and  $A_{\text{major}}$  and  $A_{\text{minor}}$  are those of major and minor enantiomers of adsorbed analyte, respectively. <sup>d</sup> Cited from ref 10. These values were determined by chromatographic separation using *M*-poly-L-1(–) chemically bonded to silica gel as the CSP. <sup>e</sup> Average values of four runs. <sup>f</sup> *M*-poly-L-1(–)-b-3 8.0 mg. <sup>g</sup> *M*-poly-L-1(–)-b-3 4.0 mg. <sup>h</sup> Experimental conditions: *M*-poly-L-1(–)-b-3 film 0.5 mg; analyte 0.41 mg (7.5 mL portion from a 0.055 mg/mL solution in toluene). <sup>i</sup> Determined by absorption spectra of the supernatant solution. <sup>j</sup> Determined by CD spectra of the supernatant solution (see Figure S2). <sup>k</sup> Experimental conditions: *M*-poly-L-1(–) chemically bonded to silica gel 13 mg; analyte 1.1 mg (20 mL portion from a 0.055 mg/mL solution in toluene).

prior to the enantioselective adsorption experiments. A solution of racemic *trans*-stilbene oxide (4) in a hexane–2-propanol mixture (98:2, v/v) (0.025 mg/mL, 200  $\mu$ L) was added to a screw-capped sample bottle containing the star polymer. A small amount of the supernatant solution was withdrawn after stirring for 2 h and analyzed by a chiral HPLC using a Daicel Chiralcel OD-H column (25 cm  $\times$  0.46 cm (i.d.)) equipped with UV and polarimetric detectors to determine the concentration and *ee* of the analyte in the supernatant. The results are summarized in Table 1. Separation factor ( $\alpha$ ) was calculated according to  $\alpha = (F_{\text{major}}(\%)/F_{\text{minor}}(\%))/(A_{\text{major}}(\%)/A_{\text{minor}}(\%))$ , where  $F_{\text{major}}$  and  $F_{\text{minor}}$  are the percentages of major and minor enantiomers of free analyte in the supernatant solution, respectively, and  $A_{\text{major}}$  and  $A_{\text{minor}}$  are those of major and minor enantiomers of adsorbed analyte, respectively.<sup>18</sup>

**Typical Procedure for Helix-Sense Selective Adsorption of Helical Poly(phenyl isocyanide)s with Macromolecular Helicity Memory.** A solution of *M*-poly-L-1(–)-b-3 in chloroform (500  $\mu$ L, 1.0 mg/mL) was placed in a sample bottle with a screw cap. Chloroform was removed by evaporation to produce the *M*-poly-L-1(–)-b-3 film, and the resulting film was dried in vacuo. A toluene solution containing an equal amount of *P*-poly-7(+) and *M*-poly-7(–) (7.5 mL, 0.055 mg/mL) was added to a screw-capped sample bottle containing the star polymer film. A small amount of the solution was withdrawn at appropriate time intervals, and the UV–vis and CD spectra of the supernatant solution were measured at 25  $^{\circ}$ C to estimate the amount and helical sense excess of the polymer analytes adsorbed on the star polymer film (Figure S2). The helical sense (*P* or *M*) and helical sense excess of the free analytes in the supernatant solution were determined by comparison of the sign and anisotropy factor, *g* value ( $\Delta\epsilon/\epsilon$ ), of the first Cotton effect to those of *M*-poly-L-1(–), whose helical sense and helical sense excess had been directly determined by high-resolution AFM observations.<sup>8,11</sup> The results are summarized in Table 1 (run 4).

**AFM Measurements of Individual Polymers and Star Polymers on Mica.** Stock solutions of *M*-poly-L-1(–)-b-3 and *M*-poly-L-1(–) in chloroform (0.001 mg/mL) were prepared. Samples for the AFM measurements were prepared by casting 7  $\mu$ L aliquots of the stock solutions of the polymers on a freshly cleaved mica, the solution was blown off simultaneously with a stream of nitrogen, and then the mica substrate was dried in vacuo overnight to measure the AFM images. The AFM measurements were performed using a Nanoscope IIIa microscope in air at ambient temperature with standard silicon cantilevers in the tapping mode. The typical settings of the AFM observations were as follows: a free amplitude of the oscillation frequency of ca. 1.0–1.5 V, a set-point amplitude

of 0.8–1.3 V, and a scan rate of 1.5 Hz. The Nanoscope image processing software was used for the image analysis. Polymer diameters were measured using the Image J program, developed at the National Institutes of Health.

**AFM Measurements of 2D Assembled *M*-Poly-L-1(–)-b-3 on HOPG.** A stock solution of *M*-poly-L-1(–)-b-3 in chloroform (0.02 mg/mL) was prepared. Samples for the AFM measurements of *M*-poly-L-1(–)-b-3 were prepared by casting 15  $\mu$ L aliquots of the stock solution on a freshly cleaved HOPG at room temperature (ca. 25  $^{\circ}$ C), and the solvents were then slowly evaporated under a chloroform vapor atmosphere. After the polymer had been deposited on the HOPG, the HOPG substrates were exposed to chloroform vapors at room temperature for 12 h, and the substrates were then dried under vacuum for 2 h. The organic solvent vapors were prepared by putting 1 mL of chloroform into a 2 mL flask that was inside a 50 mL flask, and the HOPG substrates were then placed in the 50 mL flask. The typical settings of the AFM for the high-magnification observations were as follows: a free amplitude of the oscillation frequency of ca. 1.0–1.5 V, a set-point amplitude of 0.9–1.4 V, and a scan rate of 2.5 Hz.

## ■ ASSOCIATED CONTENT

**Supporting Information.** Experimental details in the synthesis and characterization of 3 and *P*- and *M*-poly-7, CD and absorption spectral changes of *P*/*M*-poly-7 in the presence of star polymers, SEC-MALS and DLS measurement results, and histograms of the size and height distributions of star polymers obtained from the AFM images. This material is available free of charge via the Internet at <http://pubs.acs.org>.

## ■ AUTHOR INFORMATION

### Corresponding Author

\*E-mail: [yashima@apchem.nagoya-u.ac.jp](mailto:yashima@apchem.nagoya-u.ac.jp).

## ■ ACKNOWLEDGMENT

We are deeply grateful to Professor K. Onitsuka (Osaka University) for his generous supply of the Pt–Pd catalyst (2). This work was supported in part by Grant-in-Aid for Scientific Research (S) (E.Y.) and Grant-in-Aid for Young Scientists (B) (H.I.) from the Japan Society for the Promotion of Science (JSPS) and the Global COE Program “Elucidation and Design of Materials and Molecular Functions” of the Ministry of

Education, Culture, Sports, Science, and Technology, Japan. T. M. and M.B. express their thanks for JSPS Research Fellowships for Young Scientists (no. 3247 and no. 9164, respectively).

## REFERENCES

- (1) (a) Hadjichristidis, N.; Pitsikalis, M.; Pispas, S.; Iatrou, H. *Chem. Rev.* **2001**, *101*, 3747–3792. (b) Blencowe, A.; Tan, J. F.; Goh, T. K.; Qiao, G. G. *Polymer* **2009**, *50*, 5–32. (c) Gao, H.; Matyjaszewski, K. *Prog. Polym. Sci.* **2009**, *34*, 317–350. (d) Ouchi, M.; Terashima, T.; Sawamoto, M. *Chem. Rev.* **2009**, *109*, 4963–5050. (e) Rosen, B. M.; Percec, V. *Chem. Rev.* **2009**, *109*, 5069–5119. (f) Aoshima, S.; Kanaoka, S. *Chem. Rev.* **2009**, *109*, 5245–5287. (g) Matyjaszewski, K.; Tsarevsky, N. V. *Nature Chem.* **2009**, *1*, 276–288.
- (2) Bosman, A. W.; Heumann, A.; Klaerner, G.; Benoit, D.; Fréchet, J. M. J.; Hawker, C. J. *J. Am. Chem. Soc.* **2001**, *123*, 6461–6462.
- (3) (a) Bosman, A. W.; Vestberg, R.; Heumann, A.; Fréchet, J. M. J.; Hawker, C. J. *J. Am. Chem. Soc.* **2003**, *125*, 715–728. (b) Chi, Y.; Scroggins, S. T.; Fréchet, J. M. J. *J. Am. Chem. Soc.* **2008**, *130*, 6322–6323. (c) Rodionov, V.; Gao, H.; Scroggins, S.; Unruh, D. A.; Avestro, A.-J.; Fréchet, J. M. J. *J. Am. Chem. Soc.* **2010**, *132*, 2570–2572.
- (4) (a) Baek, K.-Y.; Kamigaito, M.; Sawamoto, M. *Macromolecules* **2002**, *35*, 1493–1498. (b) Skey, J.; Willcock, H.; Lammens, M.; Prez, F. D.; O'Reilly, R. K. *Macromolecules* **2010**, *43*, 5949–5955. (c) Koda, Y.; Terashima, T.; Nomura, A.; Ouchi, M.; Sawamoto, M. *Macromolecules* **2011**, *44*, 4574–4578.
- (5) For optically active multiarmed star polymers, see refs 3b and 3c. For optically active star polymers carrying flexible 3 or 4 arms, see: (a) Angiolini, L.; Benelli, T.; Giorgini, L.; Salatelli, E. *Macromolecules* **2006**, *39*, 3731–3737. (b) Barberá, J.; Giorgini, L.; Paris, F.; Salatelli, E.; Tejedor, R. M.; Angiolini, L. *Chem.—Eur. J.* **2008**, *14*, 11209–11221. (c) Lou, L.; Jiang, L.; Liu, J.; Sun, W.; Shen, Z. *Polym. Int.* **2007**, *56*, 796–802. For optically active star polymers carrying rigid-rod helical 3, 4, or 6 arms, see ref 4b. (d) Wulff, G.; Zweering, U. *Chem.—Eur. J.* **1999**, *5*, 1898–1904. (e) Onitsuka, K.; Yabe, K.-i.; Ohshiro, N.; Shimizu, A.; Okumura, R.; Takei, F.; Takahashi, S. *Macromolecules* **2004**, *37*, 8204–8211. For optically star polymers carrying rigid-rod helical multiarms, see: (f) Knoop, R. J. I.; de Geus, M.; Habraken, G. J. M.; Koning, C. E.; Menzel, H.; A. Heise, A. *Macromolecules* **2010**, *43*, 4126–4132.
- (6) For reviews: (a) Nakano, T.; Okamoto, Y. *Chem. Rev.* **2001**, *101*, 4013–4038. (b) Maeda, K.; Yashima, E. *Top. Curr. Chem.* **2006**, *265*, 47–88. (c) Yashima, E.; Maeda, K. *Macromolecules* **2008**, *41*, 3–12. (d) Yashima, E.; Maeda, K.; Iida, H.; Furusho, Y.; Nagai, K. *Chem. Rev.* **2009**, *109*, 6102–6211. (e) Fujiki, M. *Chem. Rec.* **2009**, *9*, 271–298.
- (7) (a) Onitsuka, K.; Joh, T.; Takahashi, S. *Bull. Chem. Soc. Jpn.* **1992**, *65*, 1179–1181. (b) Onitsuka, K.; Joh, T.; Takahashi, S. *Angew. Chem., Int. Ed. Engl.* **1992**, *31*, 851–852.
- (8) Onouchi, H.; Okoshi, K.; Kajitani, T.; Sakurai, S.-i.; Nagai, K.; Kumaki, J.; Onitsuka, K.; Yashima, E. *J. Am. Chem. Soc.* **2008**, *130*, 229–236.
- (9) For reviews of helical polyisocyanides, see: (a) Cornelissen, J. J. L. M.; Rowan, A. E.; Nolte, R. J. M.; Sommerdijk, N. A. J. M. *Chem. Rev.* **2001**, *101*, 4039–4070. (b) Sugimoto, M.; Ito, Y. *Adv. Polym. Sci.* **2004**, *17*, 77–136. (c) Amabilino, D. B.; Serrano, J.-L.; Sierra, T.; Veciana, J. J. *Polym. Sci., Part A: Polym. Chem.* **2006**, *44*, 3161–3174. (d) Schwartz, E.; Koepf, M.; Kitto, H. J.; Nolte, R. J. M.; Rowan, A. E. *Polym. Chem.* **2011**, *2*, 33–47.
- (10) With their well-defined one-handed helical structures, the P- and M-poly-L-1s resolved a variety of racemic compounds into enantiomers when used as a chiral stationary phase (CSP) for HPLC. Tamura, K.; Miyabe, T.; Iida, H.; Yashima, E. *Polym. Chem.* **2011**, *2*, 91–98.
- (11) (a) Wu, Z.-Q.; Nagai, K.; Banno, M.; Okoshi, K.; Onitsuka, K.; Yashima, E. *J. Am. Chem. Soc.* **2009**, *131*, 6708–6718. (b) Banno, M.; Wu, Z.-Q.; Nagai, K.; Sakurai, S.-i.; Okoshi, K.; Yashima, E. *Macromolecules* **2010**, *43*, 6553–6561.
- (12) Okoshi, K.; Nagai, K.; Kajitani, T.; Sakurai, S.-i.; Yashima, E. *Macromolecules* **2008**, *41*, 7752–7754.
- (13) For reviews, see: (a) Schlüter, A. D.; Rabe, J. P. *Angew. Chem., Int. Ed.* **2000**, *39*, 864–883. (b) Sheiko, S. S.; Möller, M. *Chem. Rev.* **2001**, *101*, 4099–4123. (c) Magonov, N. S. In *Encyclopedia of Analytical Chemistry*; Meyers, R. A., Ed.; John Wiley: Chichester, 2000; pp 7432–7491. (d) Minko, S.; Roiter, Y. *Curr. Opin. Colloid Interface Sci.* **2005**, *10*, 9–15. (e) Samorì, P.; Surin, M.; Palermo, V.; Lazzaroni, R.; Leclère, P. *Phys. Chem. Chem. Phys.* **2006**, *8*, 3927–3938.
- (14) (a) Kiriya, A.; Gorodyska, G.; Minko, S.; Stamm, M.; Tsitsilianis, C. *Macromolecules* **2003**, *36*, 8704–8711. (b) Xue, L.; Agarwal, U. S.; Zhang, M.; Staal, B. B. P.; Müller, A. H. E.; Bailly, C. M. E.; Lemstra, P. J. *Macromolecules* **2005**, *38*, 2093–2100. (c) Huang, J.; Jia, S.; Siegwart, D. J.; Kowalewski, T.; Matyjaszewski, K. *Macromol. Chem. Phys.* **2006**, *207*, 801–811. (d) Kreutzer, G.; Ternat, C.; Nguyen, T. Q.; Plummer, C. J. G.; Månson, J.-A. E.; Castelletto, V.; Hamley, I. W.; Sun, F.; Sheiko, S. S.; Herrmann, A.; Ouali, L.; Sommer, H.; Fieber, W.; Velazco, M. I.; Klok, H.-A. *Macromolecules* **2006**, *39*, 4507–4516. (e) Amamoto, Y.; Higaki, Y.; Matsuda, Y.; Otsuka, H.; Takahara, A. *J. Am. Chem. Soc.* **2007**, *129*, 13298–13304.
- (15) (a) Matyjaszewski, K.; Qin, S.; Boyce, J. R.; Shirvayants, D.; Sheiko, S. S. *Macromolecules* **2003**, *36*, 1843–1849. (b) Schappacher, M.; Defieux, A. *Macromolecules* **2005**, *38*, 4942–4946. For recent review, see: (c) Sheiko, S. S.; Sumerlin, B. S.; Matyjaszewski, K. *Prog. Polym. Sci.* **2008**, *33*, 759–785.
- (16) Kanaoka, S.; Sawamoto, M.; Higashimura, T. *Macromolecules* **1991**, *24*, 2309–2313.
- (17) This method is very useful for constructing highly ordered 2D helix-bundles for helical polyisocyanides, polyacetylenes, and complementary double-stranded helical polymers on HOPG, and their helical structures were visualized by AFM. See: (a) Sakurai, S.-i.; Okoshi, K.; Kumaki, J.; Yashima, E. *Angew. Chem., Int. Ed.* **2006**, *45*, 1245–1248. (b) Kajitani, T.; Okoshi, K.; Sakurai, S.-i.; Kumaki, J.; Yashima, E. *J. Am. Chem. Soc.* **2006**, *128*, 708–709. (c) Sakurai, S.-i.; Okoshi, K.; Kumaki, J.; Yashima, E. *J. Am. Chem. Soc.* **2006**, *128*, 5650–5651. (d) Sakurai, S.-i.; Ohsawa, S.; Nagai, K.; Okoshi, K.; Kumaki, J.; Yashima, E. *Angew. Chem., Int. Ed.* **2007**, *46*, 7605–7608. (e) Maeda, T.; Furusho, Y.; Sakurai, S.-i.; Kumaki, J.; Okoshi, K.; Yashima, E. *J. Am. Chem. Soc.* **2008**, *130*, 7938–7945. (f) Louzao, I.; Seco, J. M.; Quiñoá, E.; Riguera, R. *Angew. Chem., Int. Ed.* **2010**, *49*, 1430–1433. For a review, see: (g) Kumaki, J.; Sakurai, S.-i.; Yashima, E. *Chem. Soc. Rev.* **2009**, *38*, 737–746.
- (18) (a) Yashima, E.; Noguchi, J.; Okamoto, Y. *Macromolecules* **1995**, *28*, 8368–8374. (b) Nakano, T.; Satoh, Y.; Okamoto, Y. *Polym. J.* **1998**, *30*, 635–640.
- (19) (a) Ishikawa, M.; Maeda, K.; Yashima, E. *J. Am. Chem. Soc.* **2002**, *124*, 7448–7458. (b) Ishikawa, M.; Maeda, K.; Mitsutsuji, Y.; Yashima, E. *J. Am. Chem. Soc.* **2004**, *126*, 732–733. (c) Ishikawa, M.; Taura, D.; Maeda, K.; Yashima, E. *Chem. Lett.* **2004**, *33*, 550–551. (d) Hase, Y.; Ishikawa, M.; Muraki, R.; Maeda, K.; Yashima, E. *Macromolecules* **2006**, *39*, 6003–6008. (e) Hase, Y.; Mitsutsuji, Y.; Ishikawa, M.; Maeda, K.; Okoshi, K.; Yashima, E. *Chem.—Asian. J.* **2007**, *2*, 755–763. (f) Miyabe, T.; Hase, Y.; Iida, H.; Maeda, K.; Yashima, E. *Chirality* **2009**, *21*, 44–50. (g) Hase, Y.; Nagai, K.; Iida, H.; Maeda, K.; Ochi, N.; Sawabe, K.; Sakajiri, K.; Okoshi, K.; Yashima, E. *J. Am. Chem. Soc.* **2009**, *131*, 10719–10732.
- (20) Kaida, Y.; Okamoto, Y. *Bull. Chem. Soc. Jpn.* **1992**, *65*, 2286–2288.